Carbohydrate Polymers 86 (2011) 94–104

Contents lists available at ScienceDirect

Carbohydrate Polymers

journal homepage: www.elsevier.com/locate/carbpol

Blends of cellulose and poly(3-hydroxybutyrate-co-3-hydroxyvalerate) prepared from the ionic liquid 1-butyl-3-methylimidazolium chloride

Nishar Hameed [a], Qipeng Guo [a,*], Feng H. Tay [b], Sergei G. Kazarian [b]

[a] Institute for Technology, Research and Innovation, Deakin University, Geelong, Victoria 3217, Australia
[b] Department of Chemical Engineering, Imperial College London, SW7 2AZ, UK

ARTICLE INFO

Article history:
Received 17 December 2010
Received in revised form 6 April 2011
Accepted 8 April 2011
Available online 15 April 2011

Keywords:
Cellulose
PHBV
Blends
Ionic liquid
FT-IR imaging

ABSTRACT

We report blends of cellulose and a microorganism-synthesized biopolymer, namely poly(3-hydroxybutyrate-co-3-hydroxyvalerate) (PHBV) copolymer prepared from an ionic liquid solvent, 1-butyl-3-methylimidazolium chloride. The ionic liquid was completely recycled with high yield and purity after the processing. The blends can be processed into different solid material forms such as films, noodle-like fibers and bulk blocks. These blends show phase-separated structure. The PHBV domains of 6–8 μm, as analyzed with SEM and FTIR imaging, are distributed in a cellulose matrix at high concentrations of cellulose while the blends with high PHBV concentrations exhibit multiphase morphologies, including beadlike PHBV microdomains in the range of 300–400 nm. The dispersion of PHBV in cellulose leads to significant improvement in hydrophobicity due to its beadlike structure. Cellulose is a very brittle polymer and intractable to process. The addition of PHBV reduces the Young's modulus but increases the elongation at break, considerably plasticizing cellulose.

1. Introduction

Cellulose, the structural component of the primary cell wall of green plants, is the most abundant natural polymer (Kaplan, 1998; Klemm, Heublein, Fink, & Bohn, 2005; Walker, 1993; Xie, King, Kilpelainen, Granstrom, & Argyropoulos, 2007). Cellulose is hydrophilic, biodegradable and not soluble in water or most organic solvents because of its well developed intermolecular hydrogen bonding. Cellulose exhibits desirable mechanical properties due to its highly ordered structure which however, makes it a challenge to find suitable solvents for its dissolution. All those limited number of solvent systems for dissolving cellulose have perceived harmful effects on human health, safety, and the environment combined with their volatility and flammability (Garrett & Grisham, 2002).

However, recently Swatloski, Spear, Holbrey, and Rogers (2002) reported the use of ionic liquids (ILs) as a new class of solvents both for the regeneration and chemical modification of cellulose. ILs which are molten salts with low melting temperature, are attracting much attention for potential applications in various fields due to their unique physic-chemical properties such as non-volatility, non-flammability, chemical and thermal stability and ease of recycling (Davis & Fox, 2003; Dupont, de Souza, & Suarez, 2002; Earle & Seddon, 2000; Huddleston et al., 2001; Kazarian, Sakellarios, & Gordon, 2002; Sheldon, 2001; Song, 2004; Ueki & Watanabe, 2008; Wasserscheid & Keim, 2000; Welton, 1999; Zhang et al., 2006). In fact, the properties of ILs can be manipulated according to the requirements since they offer great flexibility in designing cationic and anionic structures and their combinations; therefore they have been termed the "designers solvent" (Ueki & Watanabe, 2008). ILs possess exceptional solubility characteristics due to their special structures compared to the traditional molecular solvents. Swatloski et al. (2002) showed that cellulose can be easily dissolved in ILs without the formation of any derivatives. They prepared concentrated solutions of cellulose in 1-butyl-3-methylimidazolium chloride (BMIMCl) and cellulose can be regenerated by coagulation in water or ethanol. 1-Allyl-3-methylimidazolium chloride (AMIMCl) is another highly efficient direct cellulose solvent developed by Zhang et al. (Wu et al., 2004; Zhang et al., 2007; Zhang, Wu, Zhang, & He, 2005) and they found that regenerated cellulose from AMIMCL exhibited good mechanical properties.

Many recent studies have been reported on the dissolution and regeneration of cellulose in different ILs (Kadokaw, Murakami, Takegaw, & Kaneko, 2009; Swatloski et al., 2002; Wu, Wang, Li, Li, & Wang, 2009a, 2009b; Wu et al., 2004; Zhang et al., 2007, 2005). Even though the efficacy of IL as a medium for the blending of natural polymers was indicated, to date research with natural polymers and ILs has largely focused on single component natural polymers. Very recently, Hameed and Guo (2009, 2010) successfully developed the blends of natural polymers such as wool and cellulose using room temperature ionic liquid as the solvent media. In this paper, we

* Corresponding author.
E-mail address: qguo@deakin.edu.au (Q. Guo).

0144-8617/$ – see front matter © 2011 Elsevier Ltd. All rights reserved.
doi:10.1016/j.carbpol.2011.04.016

report the development of a class of biorenewable plastics by blending cellulose with poly(3-hydroxybutyrate-co-3-hydroxyvalerate) (PHBV) copolymer using BMIMCl as the solvent media. Among the family of bacterial polyhydroxyalkanoates, PHBV copolymer is an important eco-friendly biopolymer, commercialized under the trade name of BIOPOL® as a substitute for non-biodegradable conventional plastics (Lee, 1996; Sankhla, Bhati, Singh, & Mallick, 2010). Like cellulose, PHBV can also be dissolved and regenerated in BMIMCl. In this work, we investigate how the intractable natural polymer cellulose can be blended with PHBV using the IL solvent BMIMCl to produce biorenewable plastics in different solid forms such as films, noodle-like fibers and bulk blocks. Cellulose and PHBV were blended together in BMIMCl to study the miscibility and hydrogen bonding interactions between these two polymers and also to examine the phase separated morphologies in these blends. These blends can be potentially used for the preparation of biodegradable films and fibers. The structure and morphology in these blends are studied by scanning electron microscopy, infrared spectroscopic imaging and wide-angle X-ray diffraction. We also investigate the hydrogen bonding interactions, thermal and mechanical properties and improvement in surface hydrophobicity of the blends.

2. Experimental

2.1. Materials and preparation of samples

Poly(3-hydroxybutyrate-co-3-hydroxyvalerate) (PHBV) copolymer of natural origin with PHV content 12 wt% is a product from Sigma Aldrich. Microgranular cellulose was also purchased from Sigma Aldrich. The cellulose and PHBV samples were dried at 80 °C under vacuum for about 5 h to remove moisture. 1-Butyl-3-methylimidazolium chloride (BMIMCl) was obtained from Fluka. All the materials were used as received.

The regenerated cellulose, PHBV, and the blends were prepared in the following way. The processing steps are shown in Scheme 1. To dissolve cellulose, 1 g of cellulose was mixed with 20 mL BMIMCl (melted by heating to 70 °C), heated and stirred at 100 °C to obtain a 5 wt% completely homogeneous cellulose solution. To obtain 5 wt% of PHBV solution in BMIMCl, about 1 g of PHBV was dispersed into 20 mL of BMIMCl in a 100 mL flask, and the mixture was heated at 100 °C and stirred until PHBV was completely dissolved in 5 hrs to give a clear and viscous solution. The dissolved cellulose and PHBV could be coagulated in water as BMIMCl was completely miscible with water in any ratios. This was conducted by pouring the viscous solution into excess of deionized water and coagulated several times. The mixture solutions were prepared by the mutual mixing of cellulose/BMIMCl and PHBV/BMIMCl solutions together. This was done by taking different weight ratios of cellulose and PHBV in BMIMCl, dissolved them individually and mixed with each other. The mixture solution was stirred at 100 °C again for 12 h in order to ensure the complete intermixing. Regenerated cellulose/PHBV blends were obtained in the same way as that of regenerated cellulose.

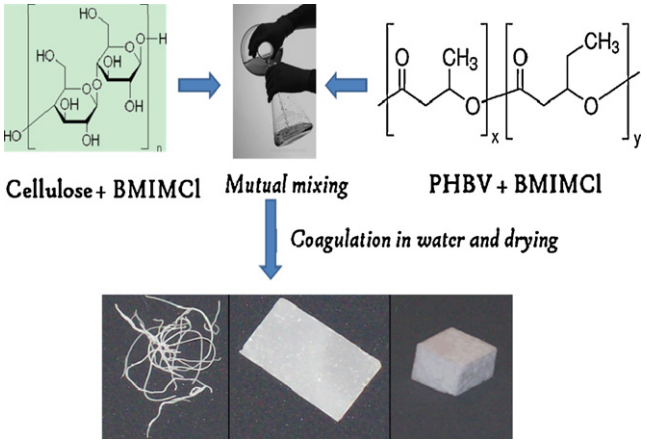

Scheme 1. The processing steps in the preparation of cellulose/PHBV blends.

The dissolved cellulose, PHBV and the blends can be regenerated as films, noodle-like fibers and rectangular blocks. The films were obtained by casting the viscous solution in between two glass plates and then soaked in the water bath to allow the IL to diffuse from the film. The fibers were obtained by pouring the BMIMCl solution into deionized water and remove the IL by coagulation and the blocks were obtained by taking the solution in rectangular moulds followed by the removal of the IL. During the process, water should be changed several times to ensure that the IL is removed completely from the sample. After washing with deionized water several times for the complete removal of the BMIMCl, the regenerated cellulose and PHBV films, fibers and blocks were dried in a vacuum oven for 72 h. The samples of blends with compositions of 20/80, 40/60, 50/50, 60/40, 80/20 cellulose/PHBV were prepared.

2.2. Characterization

2.2.1. Fourier-transform infrared (FTIR) spectroscopic imaging

The FTIR imaging system used in this study consisted of a continuous scan infrared spectrometer (Varian 7000 FT-IR from Varian Inc.) incorporated with an infrared microscope (Varian UMA 600) and a 64 × 64 focal point array (FPA) detector. The FTIR images were obtained in attenuated total reflection (ATR) mode using a germanium crystal which has a refractive index of 4. The spectra were collected with a spectral range of 4000–900 cm^{-1} at 8 cm^{-1} spectral resolution with 100 co-additions. The micro ATR measurements, as it was demonstrated before (Kazarian, Chan, & Tay, 2009; Kazarian & Chan, 2010), to have an image size of ca. 63 μm × 63 μm and a spatial resolution ca. 2–4 μm. The details of this micro ATR-FTIR spectroscopic imaging approach has been described elsewhere (Kazarian et al., 2009). The sampling procedure for the micro ATR-FTIR approach is generally simple; the measured area of interest is selected using the visible microscope, and the stage is raised to bring the sample in contact with the germanium crystal for the measurement.

2.2.2. FTIR spectroscopy

The FTIR spectra of all the samples were measured on a Bruker Vertex-70 FTIR spectrometer. The KBr disk method was adopted to conduct the FTIR experiments. The sample was mixed with KBr powder, ground well and prepared to KBr disks. The disks were dried under vacuum in an oven at 100 °C before the measurements. The spectra were recorded at the average of 32 scans in the standard wavenumber range of 400–4000 cm^{-1} at a resolution of 4 cm^{-1}.

2.2.3. Differential scanning calorimetry (DSC)

DSC experiments were carried out using a TA-DSC model Q200 instrument. The measurement was performed using 5–10 mg of the sample under an atmosphere of nitrogen gas. The samples were first heated to 100 °C and held at that temperature for 5 min to remove the thermal history. Then the samples were cooled to −50 °C at a rate of 20 °C/min, held for 5 min, and subsequently heated from −50 to 200 °C at 20 °C/min (second scan). Glass transition temperature (T_g) values were taken as the midpoint of transition in the second scan of DSC thermograms.

2.2.4. Wide-angle X-ray diffraction (WAXD) measurements

X-ray diffraction measurement was performed on a Panalytical XRD instrument. The data were recorded in the range of 2θ = 5–40°

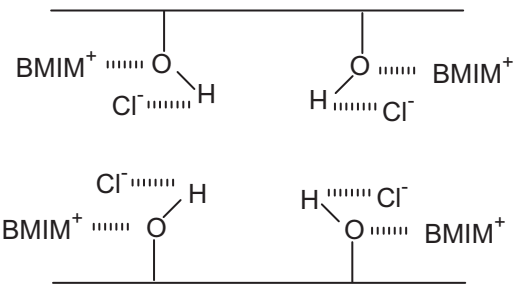

Scheme 2. Proposed dissolution mechanism of cellulose in BMIMCl.

with an X-ray diffraction. All the samples were scanned continuously with a 0.5° scan step and 1 s scan time. The regenerated film samples were cut into strips of 10 mm long and 15 mm wide for the measurements.

2.2.5. Thermogravimetric analysis (TGA)

Thermogravimetric analyses (TGA) were performed on Netzsch STA 409 thermogravimetric analyzer over a temperature range of 25–600 °C at a heating rate of 10 °C/min under nitrogen atmosphere.

2.2.6. Scanning electron microscopy (SEM)

The morphology of the blends was examined with a Leica S440 scanning electron microscope (SEM) at an activation voltage of 5 kV. The cryo-fractured and chloroform-etched surfaces were coated with thin layers of gold before the observation.

2.2.7. Mechanical tests

The tensile behavior of the blends was analyzed using a Lloyd LR 30 K testing machine in tensile mode with a load cell of 100 N capacity with a gauge length of 10 mm. The specimen was a thin rectangular strip (25 mm × 5 mm × 0.2 mm). The load–displacement curves of the samples were obtained at room temperature at a strain rate of 1 mm/min at 75% relative humidity and 20 °C temperature. The stress and strain values were obtained using the standard equations. The samples were kept at 100 °C for 15 h before the tests and experiments were repeated with 5 samples of each composition.

2.2.8. Contact angle measurements

Contact angle measurements of the blends were conducted in a KSV CAM 101 contact angle instrument. Distilled water was used for the analyses of the samples. Measurements were taken on all the samples at room temperature. The volume of the sessile drop was maintained as 1 μL in all cases using a micro-syringe. For accuracy, measurements were repeated 5–10 times on different pieces of the same sample.

3. Results and discussion

3.1. Dissolution and regeneration of cellulose using ionic liquids

1-Butyl-3-methylimidazolium chloride (BMIMCl) can be considered as a good choice for cellulose dissolution and regeneration due to its high polarity and ionic character (Abbott, Capper, Davies, Rasheed, & Tambyrajah, 2002; Feng & Chen, 2008; Ramnial, Ino, & Clyburne, 2005; Remsing, Swatloski, Rogers, & Moyna, 2006). In order to dissolve cellulose, the inter and intramolecular hydrogen bonding interactions have to be disrupted. It is reported that

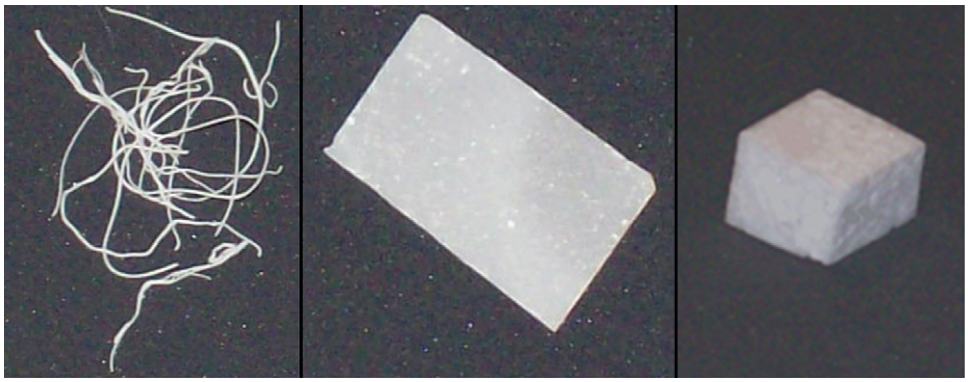

Fig. 1. Photographs of fibers, film and block of 50/50 cellulose/PHBV blend processed using the ionic liquid BMIMCl.

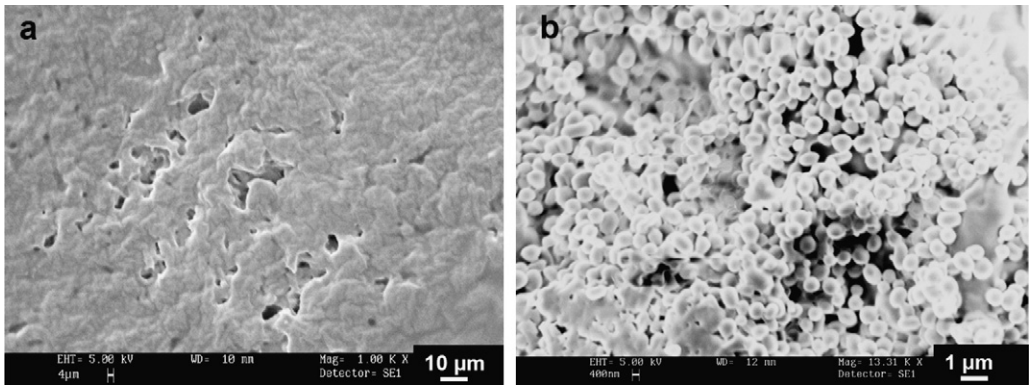

Fig. 2. Scanning electron micrographs of (a) cellulose and (b) PHBV regenerated from the ionic liquid BMIMCl.

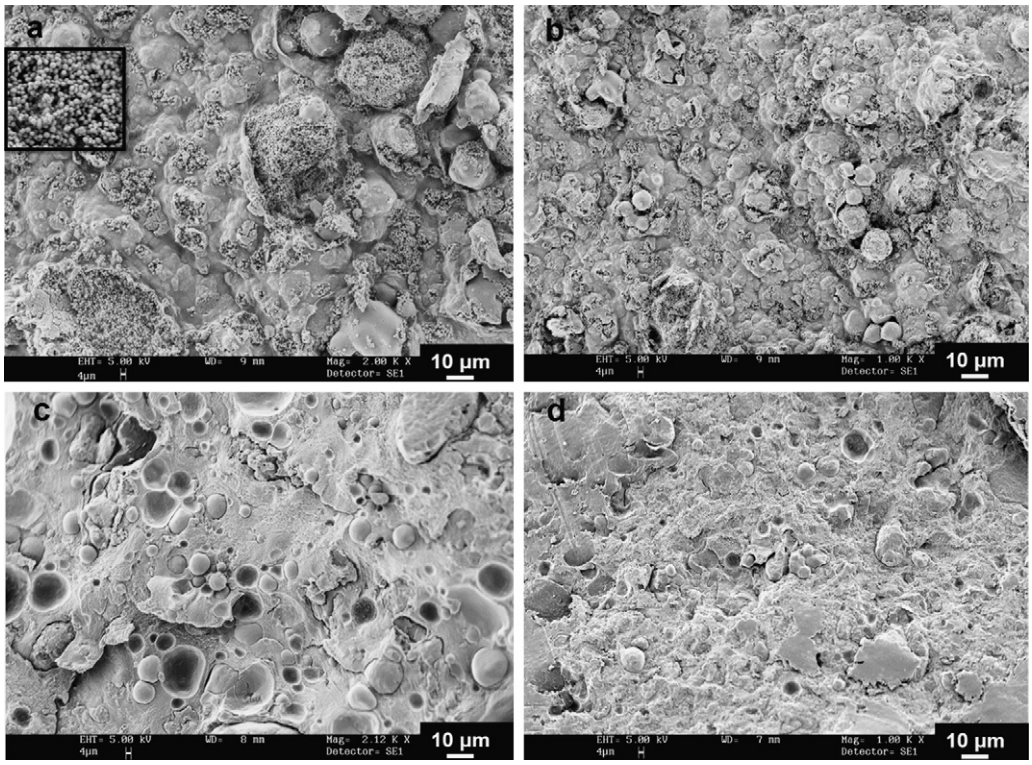

Fig. 3. Scanning electron micrographs of the cryo-fractured surfaces of (a) 20/80, (b) 40/60, (c) 60/40, and (d) 80/20 cellulose/PHBV blends.

high chloride concentration in BMIMCl is highly efficient in breaking down the networked hydrogen bonding and thereby dissolving cellulose as shown in Scheme 2 (Swatloski et al., 2002). For the regeneration of dissolved cellulose, cellulose-IL solution is precipitated with the addition of an excess of a polar solvent like water, acetone, dichloromethane, acetonitrile, or mixtures of them (Dadi, Varanasi, & Schall, 2006; El Seoud, Koschella, Fidale, Dorn, & Heinze, 2007; Ibbett, Schuster, & Fasching, 2008; Swatloski et al., 2002). Generally, deionized water is preferred as the coagulated fibers show a higher degree of crystallinity, resulting in higher strength of the regenerated matrix.

3.2. Structure and morphology of blends

The photographs of 50/50 cellulose/PHBV blend film, fiber and rectangular bulk block are shown in Fig. 1. The morphology of blends was investigated first using SEM. The cryo-fractured surface morphology of both regenerated cellulose and PHBV is given in Fig. 2. It can be observed that the regenerated cellulose shows a diffused texture as seen in Fig. 2a. Swatloski et al. (2002) previously revealed that the regenerated cellulose fibers showed a diffused morphology in which the fibers are fused into a conglomerate texture rather than a homogeneous film. The regenerated PHBV in Fig. 2b shows more interesting morphology like beads having size in the range of 300–400 nm. It can be believed that the PHBV was completely dissolved in BMIMCl and regenerated into fine beadlike structure during the repeated coagulation process to remove the BMIMCl.

Fig. 3 represents the SEM images of the morphology of the regenerated cellulose/PHBV blends. It can be observed that these blends are not homogeneous displaying characteristics of a phase separated structure. The cellulose-rich phase and the PHBV-rich phase can be easily distinguished in these images. The morphology of 20/80 cellulose/PHBV blend shows a phase separated structure in which the PHBV beads are distributed throughout the phase. The cellulose appears like a layer which covers the beads inside. The beads are in the same size range as seen in regenerated PHBV (Fig. 2b). A magnified view of the PHBV beads is shown in the inset of Fig. 3a. The 40/60 cellulose/PHBV blend shows more or less the same phase structure as that of 20/80 blend, however, the PHBV beads are less evenly distributed and the cellulose phase is more prominent than the previous composition. The morphology of above two compositions can be considered as a multiphase morphological structure where there are microphases with two different length scales, i.e., large PHBV microphase covered inside the cellulose layer and small beadlike microdomains with a size in the order of 300–400 nm, were found inside the large microphases. The 60/40 cellulose/PHBV blend shows a conventional phase separated morphology in which the spherical PHBV microphase is distributed throughout the cellulose matrix phase as seen in Fig. 3c. Interestingly the beadlike structure is absent for the PHBV phase in this composition. In 80/20 cellulose/PHBV blend (Fig. 3d), the morphology is more or less homogeneous except for a very few small sized PHBV spherical particles in the cellulose. The morphology of cellulose/PHBV blends was again observed using SEM after etching in chloroform. The SEM images are given in Fig. 4. It can be seen that the PHBV phase was completely removed after etching. The size of the microphases varies with different compositions.

The morphology of blends was further investigated using FTIR spectroscopic imaging. FTIR spectroscopic imaging offers the possibility to combine spectral and spatial information, thereby enabling a chemical visualization of samples, particularly in ATR-FTIR imaging mode. It has been applied to various areas such as in polymers (Gupper & Kazarian, 2005; Gupper et al., 2002; Kazarian & Chan, 2004), biomedical materials (Chan, Kazarian, Mavraki, & Williams, 2005; Kazarian & Chan, 2006; Kuimova, Chan, & Kazarian, 2009; Palombo, Shen, Benguigui, Kazarian, & Upmacis, 2009), crude oil fouling (Tay & Kazarian, 2009), cultural heritage and conservation studies (Spring, Ricci, Peggie, & Kazarian, 2008).

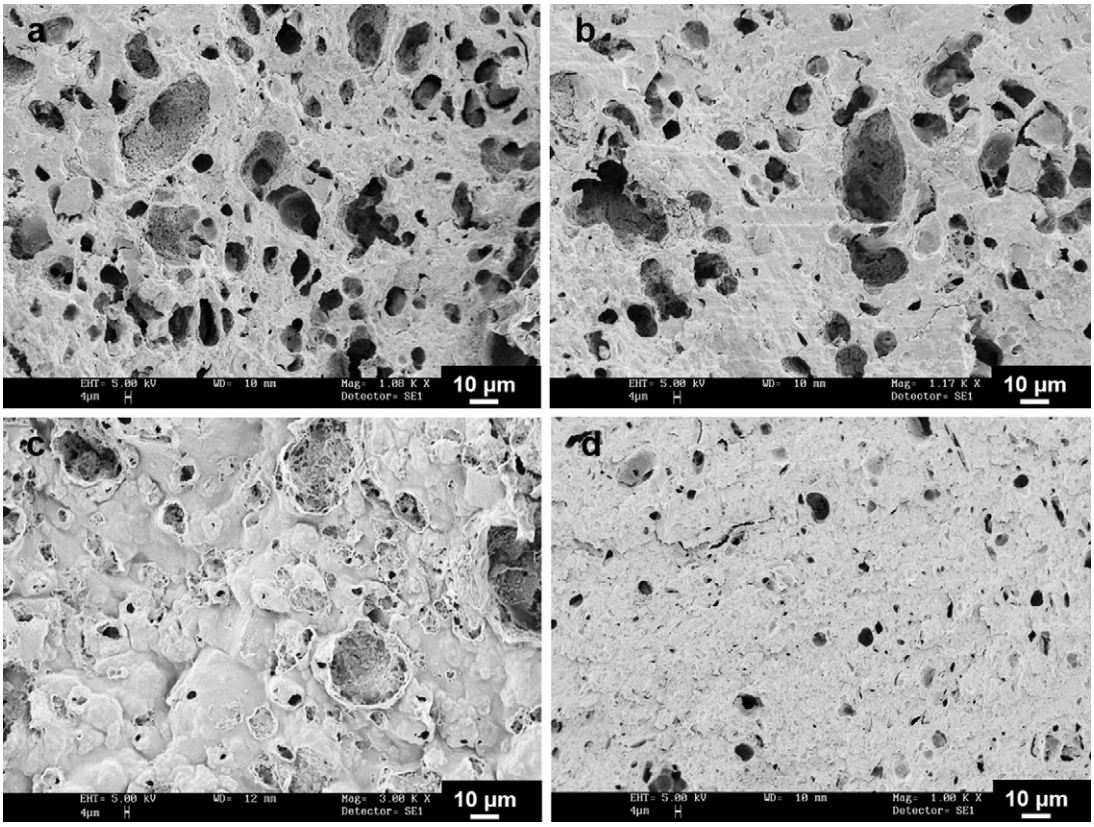

Fig. 4. Scanning electron micrographs of the chloroform-etched surfaces of (a) 20/80, (b) 40/60, (c) 60/40, and (d) 80/20 cellulose/PHBV blends.

In ATR-FTIR spectroscopic imaging, it is important to identify characteristic spectral bands of each component in order to construct images to show the distribution of the different components in the sample. The characteristic band of PHBV used in this study is the ν(C=O) band at 1730 cm^{-1} and the characteristic band of cellulose used is the ν(C–O–C) band at 1030 cm^{-1}. A chemical image is then generated from the data of a single measurement by allocating a color to each pixel of the FPA detector based on the integrated absorbance of the characteristic spectral range. Hence, according to the Beer-Lambert law, the image obtained represents the relative concentration of the component in the imaged area. The red on the color scale represents a high concentration and the blue on the color scale represents a low concentration of the respective component. Fig. 5 shows the spatial distribution of (a) PHBV and (b) cellulose

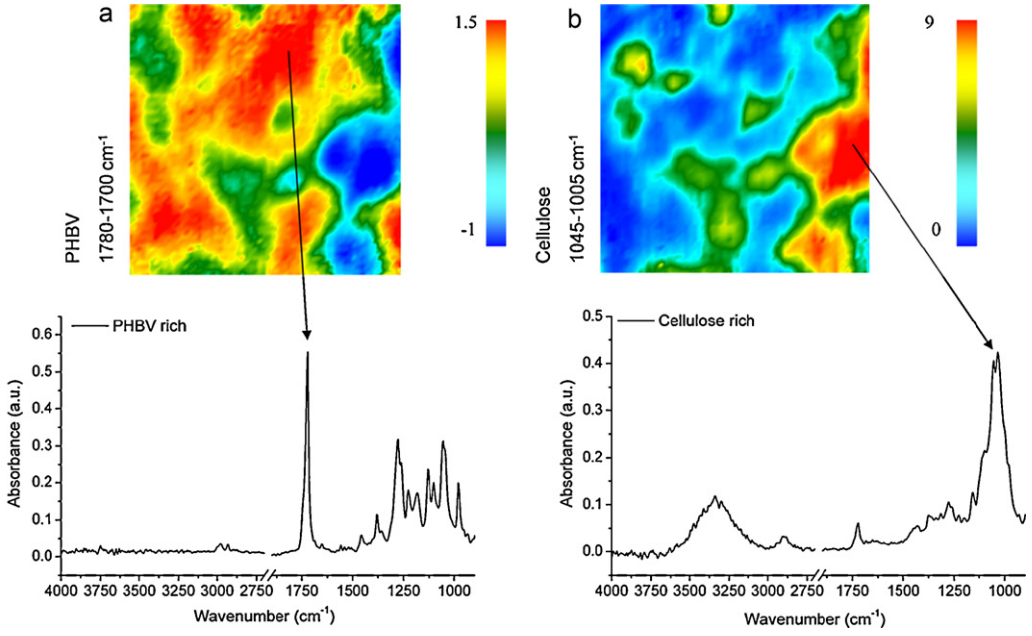

Fig. 5. Micro ATR-FTIR images of cellulose and PHBV. Image *a* is based on the spectral band of PHBV while image *b* is based on the spectral band of cellulose. The size of each image is ca. 63 μm × 63 μm.

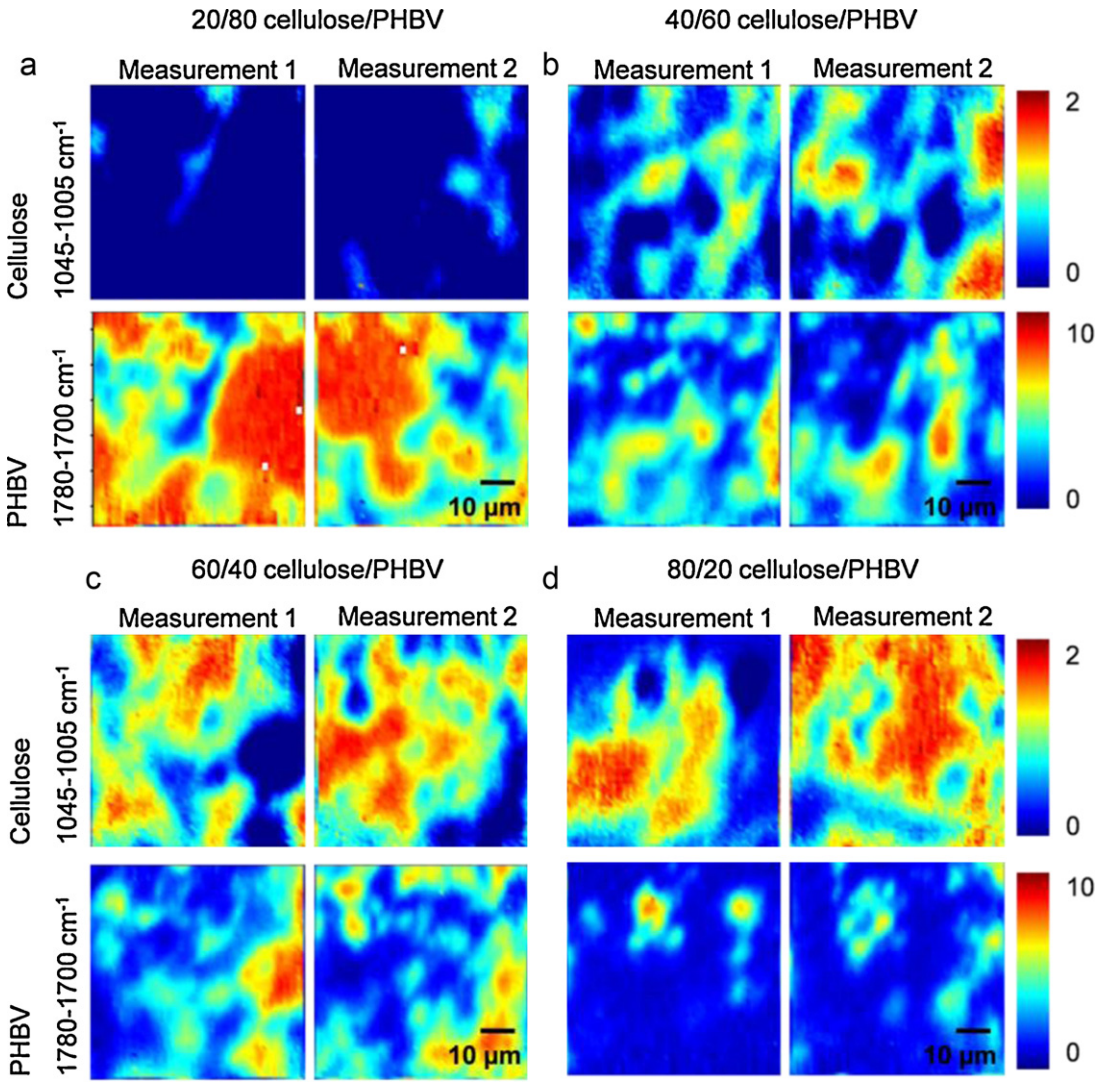

Fig. 6. Micro ATR-FTIR images of cellulose/PHBV blends at different compositions. Cellulose/PHBV: (a) 20/80, (b) 40/60, (c) 60/40, and (d) 80/20. The size of each image is ca. 63 μm × 63 μm.

components in the 60/40 cellulose/PHBV blend based on the spectral range of 1780–1700 cm^{-1} and 1045–1005 cm^{-1}, respectively. From the images of the cellulose/PHBV blends (Fig. 6), it can be observed that the cellulose-rich regions and PHBV-rich regions can be easily identified from the images corresponding to each phase and the two images complement with each other. In this imaging approach, the full mid infrared spectrum of the blend is acquired hence spectrum from domains of interest, such as the PHBV-rich region and cellulose-rich region shown in Figs. 5 and 6, can be extracted from the chemical images and analyzed.

3.3. Hydrogen bonding interactions

Cellulose is derived from D-glucose units, which condense through glycosidic bonds (Crawford, 1981; Updegraff, 1969). The multiple hydroxyl groups on the glucose residues holding the chains firmly together side-by-side and forming microfibrils with high tensile strength. The three-dimensional structure of cellulose involves intermolecular hydrogen, ionic, and physical forces of attraction. The BMIMCl is highly efficient in breaking the hydrogen bonding and dissolving these natural polymers. Both cellulose and PHBV contains many functional groups where both proton accepting and donating groups present. The ions in BMIMCl form complexes with cellulose hydroxyl group and that would disrupt the hydrogen bonding and lead to the dissolution of cellulose in BMIMCl solution. A homogeneous solution is formed upon the mutual mixing of cellulose/BMIMCl and PHBV/BMIMCl. The relatively good interaction in this composition can be expected due to the increased capability of the two polymers, cellulose with abundant hydroxyl groups and PHBV with carbonyl groups to interact mutually through hydrogen bonding.

FTIR spectroscopy has been used to prove the existence of hydrogen bonding interactions in the blends. Scheme 3 shows the possible hydrogen bonding interactions between cellulose and PHBV components. Infrared studies show that the carbonyl peaks undergo important changes, which can be attributed to the intermolecular hydrogen bonding. The carbonyl region ranging from 1850 to 1650 cm^{-1} in the IR spectra of cellulose/PHBV blends at room temperature is presented in Fig. 7a. The spectrum of regenerated PHBV shows a sharp peak at 1724 cm^{-1} and a shoulder band at 1745 cm^{-1} corresponding to PHBV crystalline and amorphous states, respectively. In cellulose/PHBV blends, as the concentration of cellulose increases, both the crystalline and amorphous peaks decrease in intensity. A new band at 1711 cm^{-1} is observed in 60/40 and 80/20 cellulose/PHBV blends which can be attributed to the vibration of the hydrogen-bonded PCL carbonyl groups. This result

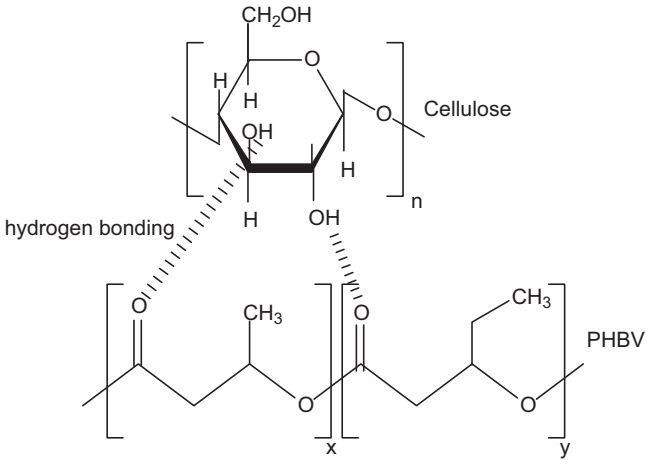

Scheme 3. Possible hydrogen bonding interaction between cellulose and PHBV.

is comparable with the FTIR bands observed by Iriondo, Iruin, and Fernandez-Berridi (1995) in PHBV/poly (vinyl phenol) blends and by Fei et al. (2004) in bisphenol A-modified PHBV. It can be noticed that the intensity of the hydrogen bonded carbonyl band is very less compared to the crystalline and amorphous bands. This is due to the small fraction of hydrogen-bonded PHBV carbonyl groups with cellulose hydroxyl groups.

The hydrogen bonding formation between cellulose and PHBV was also examined at 180 °C, above the melting point of PHBV and the corresponding IR spectra is given in Fig. 7b. The regenerated PHBV shows a single peak at 1745 cm^{-1}, corresponding to the amorphous conformation. The crystalline peak which was observed at 1724 cm^{-1} in the carbonyl region at room temperature (Fig. 7a) is not visible here because of the melting of the crystalline component of PHBV at 150 °C. For cellulose/PHBV blends, the hydrogen bonded carbonyl bands can only be observed in 60/40 and 80/20 cellulose/PHBV blends. The fraction of free carbonyl bands (1745 cm^{-1}) is comparatively very high even at very high cellulose compositions.

The quantitative study of fraction of hydrogen-bonded carbonyl groups can be performed with the variation in composition. The fraction of hydrogen-bonded carbonyl groups can be calculated using the equation (Salim, Hameed, & Guo, 2009; Salim, Hanley, & Guo, 2010);

$$f_b = \frac{A_b/a}{A_b/a + A_f} \quad (1)$$

A_f and A_b are the peak areas of the free and hydrogen-bonded carbonyl groups. The conversion constant a is the specific absorption ratio of the above two bands. The value of $a = 1.5$ for hydrogen bonded carbonyl groups (Hameed, Salim, & Guo, 2009). The results from curve fitting at 180 °C are summarized in Table 1. These results indicate that only a small fraction of carbonyl groups forms hydrogen bonds with cellulose and a major fraction of carbonyl groups exist in the free-state.

3.4. Thermal properties

The phase behavior of cellulose/PHBV blends was investigated using DSC. The DSC thermograms for the heating scan after the cooling of the blends with various compositions are shown in Fig. 8a. The T_g of cellulose in dielectric, NMR and other studies is described to be in the region 200–240 °C (Kubat & Pattyrante, 1967; Nishiyama, Langan, & Chanzy, 2002). However, T_g of regenerated cellulose could not be examined in our DSC experiments. Regenerated PHBV shows a T_g of 1 °C as can been from the figure. As the

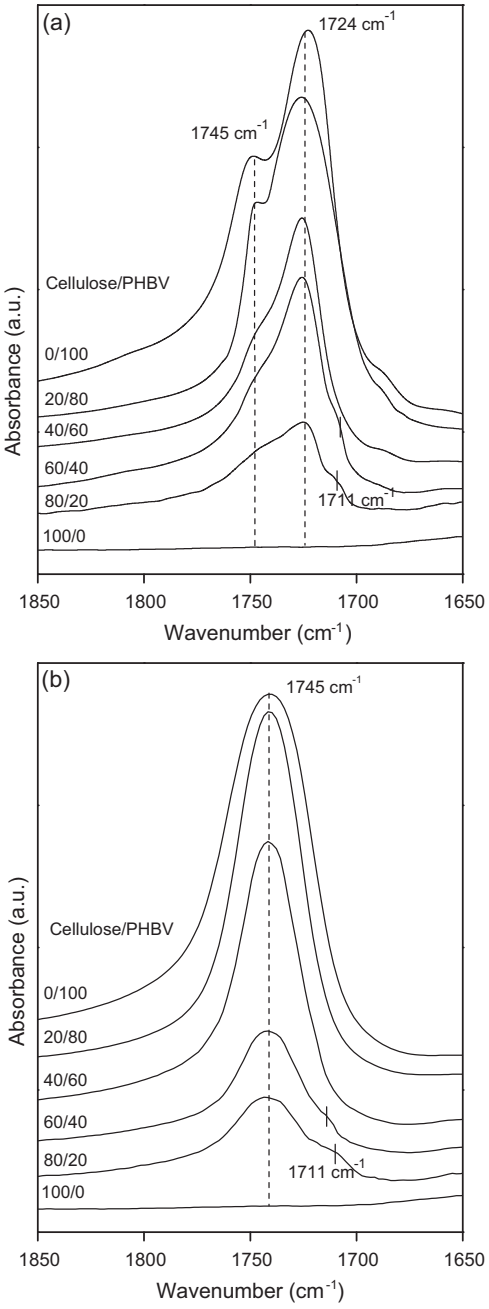

Fig. 7. Carbonyl stretching region in the infrared spectra of cellulose/PHBV blends.

concentration of cellulose increases in the blends the PHBV value shifts slightly towards higher temperatures and disappears above 60/40 cellulose/PHBV blend. This could be due to the partial miscibility of PHBV with cellulose in their regenerated form. At higher concentrations of cellulose, T_g curve disappears.

The T_g-composition diagram of the cellulose/PHBV blends is shown in Fig. 8b and the ΔH_f values are given in Table 2. The regenerated PHBV exhibits a melting peak at 149 °C which can be the crystalline PHBV phase. However, in cellulose/PHBV blends, there is a slight depression in melting point with increase in cellulose content in the blends. This can be obviously seen from the melting temperature of 80/20 cellulose/PHBV blend as 143 °C. The depression in melting point is a characteristic feature of hydrogen bonded polymer blends (Hameed & Guo, 2008; Nishiyama et al., 2002). The reduction in temperature is caused by the thermodynamic changes due to the reduction in the chemical potential. However,

Table 1
Fraction of hydrogen bonded carbonyl groups in cellulose/PHBV blends at 180 °C.

Cellulose/PHBV	Free carbonyl group			Bonded carbonyl group			f_b (%)
	υ (cm^{-1})	$W_{1/2}$ (cm^{-1})	A_f (%)	υ (cm^{-1})	$W_{1/2}$ (cm^{-1})	A_b (%)	
80/20	1745.2	15.8	86.1	1710.8	12.6	13.9	9.6
60/40	1745.7	14.3	93.4	1711.5	14.3	6.6	4.5
40/60	1745.8	18.5	100	–	–	–	–
20/80	1745.2	22. 6	100	–	–	–	–

the crystallinity of PHBV is observed in all blend compositions. This indicates that the PHBV is neither completely miscible with cellulose nor changed into amorphous state in the blends.

The X-ray diffraction studies of cellulose/PHBV blends were performed and the results are shown in Fig. 9. In regenerated cellulose, clear 2θ peaks at 14.6° and 16.2° are assigned to the [1 0 1] and [1 0 $\bar{1}$] lattice planes of cellulose I. Moreover, the peak positioned at 22° can be assigned to the [0 0 2] lattice plane of cellulose I. The regenerated PHBV shows strong peaks around 13° and 17° corresponding to the crystalline conformation of PHBV. In the blends, the diffraction peaks of crystalline PHBV were reduced, but still observed in all compositions. The cellulose and PHBV are not completely miscible and the crystallization of PHBV was not inhibited by cellulose. These results indicate that the degree of PHBV crystalline perfection becomes higher due to the lower crystallization rate under the H-bond network at higher cellulose contents. The WAXD results are consistent with the DSC experimental results.

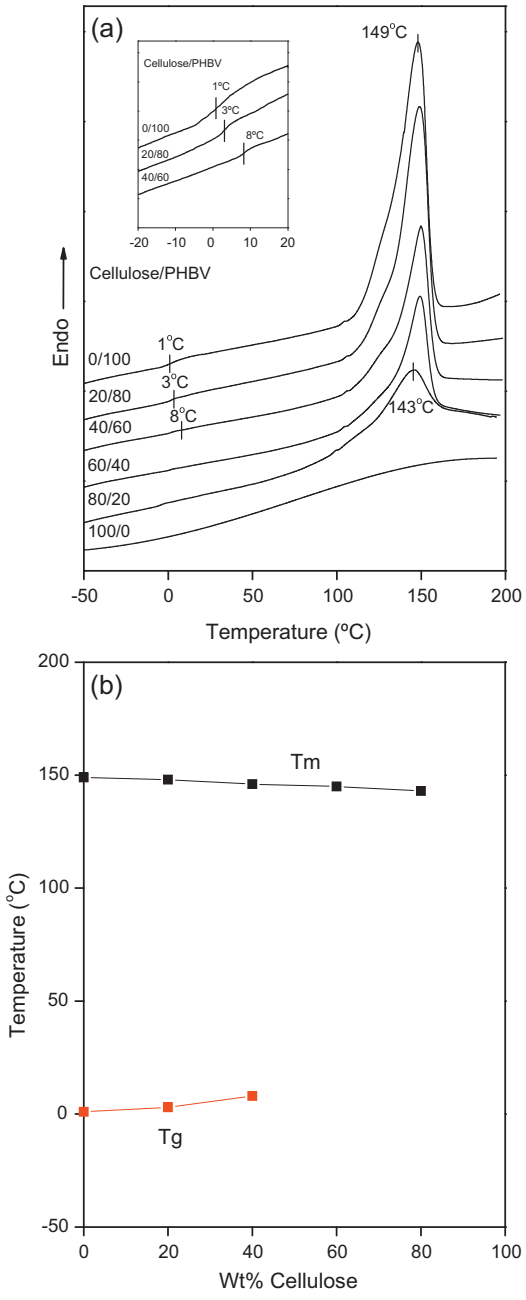

Fig. 8. (a) DSC thermograms (a magnified view of T_g region is in the inset) and (b) T_g-composition plot of cellulose/PHBV blends.

3.5. Mechanical properties and thermal stability

The stress–strain curves of cellulose/PHBV blend films regenerated from BMIMCl are shown in Fig. 10. The Young's modulus, maximum tensile strength and elongation at break are shown in Table 2. The regenerated cellulose showed highest Young's modulus value of about 2.3 GPa and the modulus is least for regenerated PHBV 0.7 GPa. Apparently the modulus gradually increased with increasing cellulose content in the blends. Tensile strength (σ_b) and elongation at break (ε_b) of the cellulose/PHBV blends mainly depend on components in the film and interfacial adhesion between them. It can be seen that the regenerated PHBV shows the lowest tensile strength of 4.4 MPa and the regenerated cellulose shows a high tensile strength ≈ 52 MPa. From Fig. 11 and Table 2, it can be observed that the tensile strength of the blends is in between the individual components. The elongation at break (ε_b) of the blends improved considerably compared to the individual components. The maximum value (ε_b = 5.2) is shown by 60/40 cellulose/PHBV blend which is 44% and 22% increment compared to regenerated PHBV and cellulose, respectively. In other words, cellulose is considerably plasticized as the

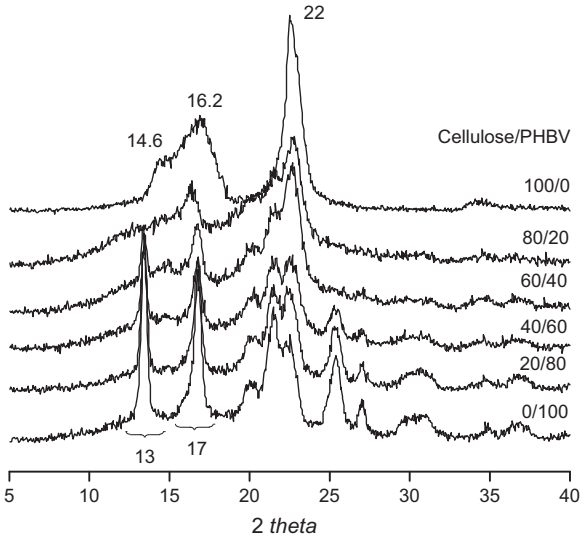

Fig. 9. WAXD patterns of cellulose/PHBV blends.

Table 2
Thermal and mechanical properties of cellulose/PHBV blends.

Cellulose/PHBV (wt%)	ΔH_f (J/g)	T_d (°C)	Young's modulus (GPa)	Tensile strength (MPa)	Elongation at break (%)
100/0	–	270	2.27 ± 0.1	52.4 ± 2.0	4.2 ± 0.6
80/20	25.15	262	2.09 ± 0.08	22.2 ± 1.3	4.5 ± 0.5
60/40	44.51	250	1.07 ± 0.05	13.8 ± 1.4	5.2 ± 0.7
40/60	60.21	248	0.98 ± 0.06	12.7 ± 1.0	4.8 ± 0.9
20/80	73.55	230	0.91 ± 0.03	7.2 ± 0.8	4.4 ± 0.1
0/100	94.18	218	0.72 ± 0.04	4.2 ± 0.5	3.6 ± 0.9

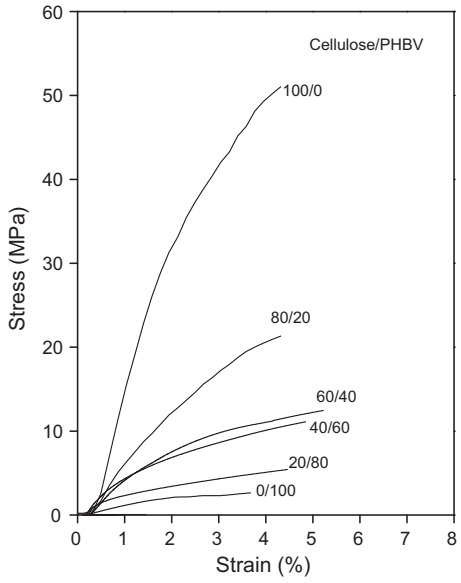

Fig. 10. Stress–strain curves of cellulose/PHBV blends.

Young's modulus is reduced with the addition of PHBV. The tensile strength shows an increasing trend with blends containing high cellulose concentration which is due to the higher strength of cellulose compared to PHBV. Though the blend is phase separated as observed from the SEM, there is a partial hydrogen bonding interaction between cellulose and PHBV which make the system more compatible.

The thermal decomposition behavior of the cellulose/PHBV blends regenerated from BMIMCl was investigated. The TGA curves of regenerated cellulose/PHBV blends are given in Fig. 11 and the decomposition temperatures are given in Table 2. The onset decomposition temperatures (T_d) of plain regenerated cellulose and PHBV are 270 °C and 218 °C, respectively. It can be observed that the blends show T_d values in between the individual components. In fact, the T_d values of cellulose/PHBV blends increases with increase in cellulose content. The enhanced thermal stability of the blends can be attributed to the strong interaction between cellulose and PHBV facilitated by the IL media as revealed by FTIR study. The char yield of the regenerated cellulose and blends containing cellulose is high due to the formation of carbonaceous materials at elevated temperature, which in fact makes a good precursor for carbon fiber (Zhang et al., 2007).

3.6. Surface properties

The change in the hydrophilic nature of the cellulose/PHBV blends with varying concentration of the components was analyzed using the water contact angle measurements. Cellulose is highly hydrophilic in nature. Toussaint and Luner (1988) reported about a rapid decrease of the contact angle of water with the time for cellulose films. Since water has a higher polarity than the other liquids, the decrease in the contact angle with the time is due to spe-

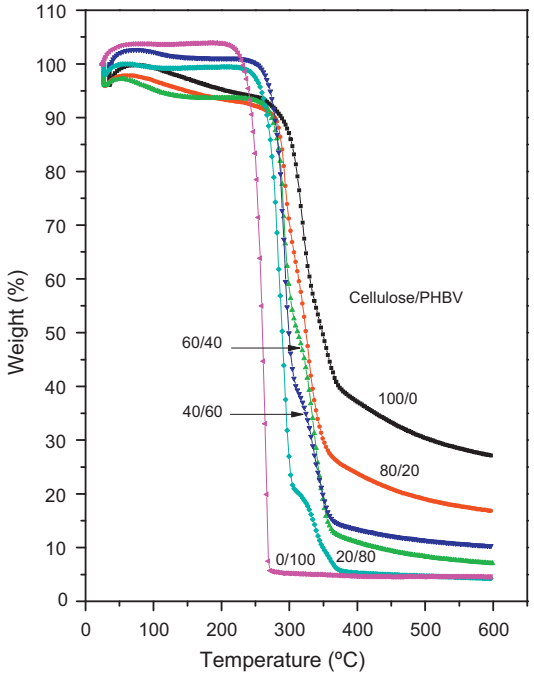

Fig. 11. TGA curves of cellulose/PHBV blends.

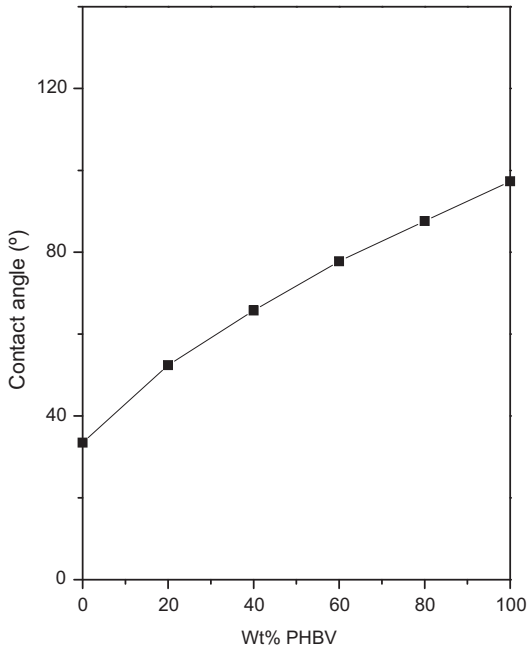

Fig. 12. Contact angle (θ) values versus composition of cellulose/PHBV blends.

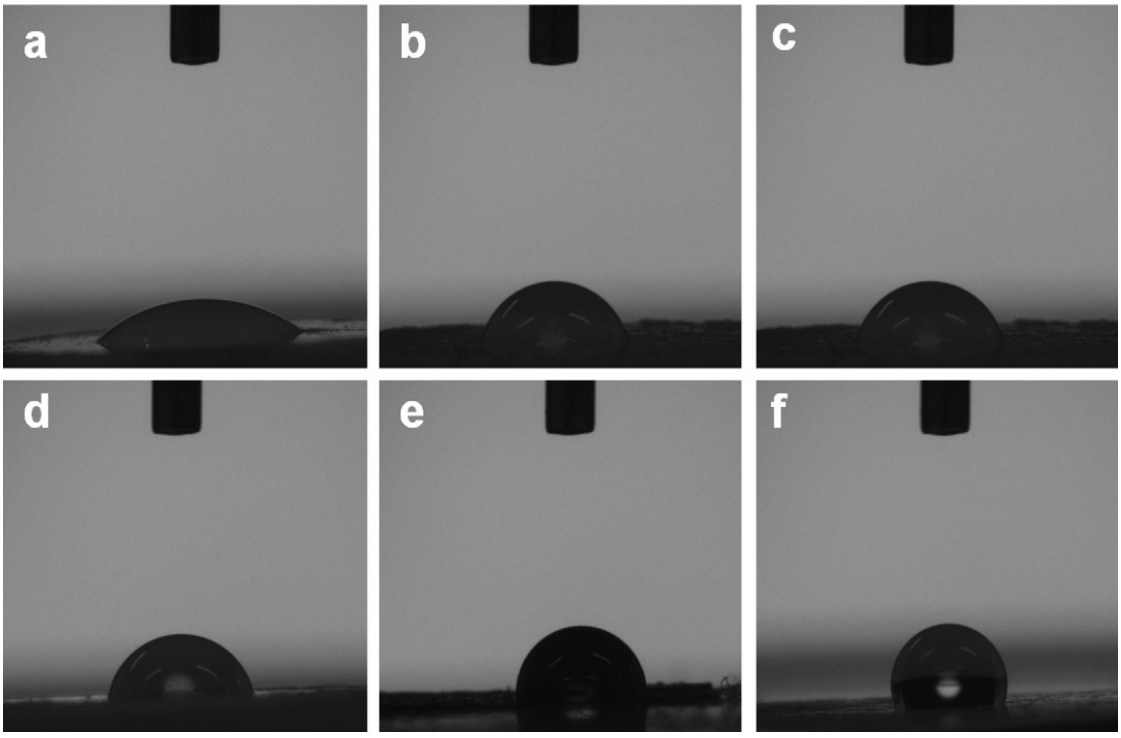

Fig. 13. Photographs of water droplets on surfaces of cellulose/PHBV blends taken during contact measurements. Cellulose/PHBV: (a) 100/0, (b) 80/20, (c) 60/40, (d) 40/60, (e) 20/80, and (f) 0/100.

cific interactions between water and the cellulose surface allowing water to penetrate into the cellulose, causing the cellulose to swell, thus lowering the interfacial free energy and decreasing the contact angle. PHBV is moderately hydrophilic in nature however; interestingly regenerated PHBV exhibits high hydrophobic characteristics. Fig. 12 shows the contact angle (θ) values of cellulose/PHBV blend films as a function of the composition. Regenerated PHBV shows an average θ value of about 97° whereas that of regenerated cellulose is just 33°. It can be observed that the blend films become more and more hydrophobic with increase in concentration of PHBV. This increase in hydrophobicity of the blend films can be observed from the photographs of water droplets on the blend film surfaces as shown in Fig. 13.

The improved hydrophobic nature of the regenerated PHBV and the blend films can be correlated with their morphology. It is clear from Fig. 2b that regenerated PHBV exhibits a beadlike structure with a size in the range of approximately 400 nm. This nature of PHBV provides high surface area which in turn results in hydrophobic surfaces. In blends containing high PHBV contents (20/80 and 40/60 cellulose/PHBV) the surface is covered with PHBV beads causes increased hydrophobicity. Moreover, it can be assumed that the intramolecular hydrogen bonding within the cellulose and intermolecular hydrogen bonding between cellulose hydroxyl groups and PHBV carbonyl groups also contribute to the reduction in surface free energy; thereby increase in contact angle value of these blends.

3.7. Ionic liquid recycling

The solvation properties of ILs can be determined by their hydrophilic/hydrophobic nature of a particular IL. The route for separating water-miscible ILs from the aqueous phase was investigated recently (Wu, Zhang, & Wang, 2008). The main factors determining the miscibility of ILs with water are the hydrophilic nature of the anion and the hydrophobic nature of the cation, which is primarily determined by the length of the alkyl chains (Chiappe & Pieraccini, 2005). Generally, the solubility of water decreases with a decrease in temperature.

After the coagulation and regeneration of cellulose/PHBV blends, the residual BMIMCl in coagulation bath was recovered by the process described by other authors (Swatloski et al., 2002; Wu et al., 2004; Zhang et al., 2005). Rotary evaporator was employed under reduced pressure to water from BMIMCl and majority amount of water can be removed by this procedure. Then freeze dryer was used to eliminate the remaining trace water.

4. Conclusions

Blends based on intractable natural polymer cellulose and bacterial PHBV copolymer can be prepared using the ionic liquid BMIMCl as the processing solvent. The blends can be processed into different solid forms such as fibers, films and bulk blocks. Morphological observations indicate that the PHBV phase is distributed in cellulose matrix at low PHBV contents whereas beadlike PHBV microdomains are formed at higher PHBV concentrations. The surface hydrophobicity of the cellulose was greatly improved by blending with PHBV. Remarkably the beadlike microdomains of PHBV in the size of 300–400 nm dispersed in the cellulose contribute to the significant improvement of hydrophobicity of the blends. There was intermolecular hydrogen bonding between regenerated cellulose and PHBV in the blends. The elongation at break of the blends was found to be higher than individual components while the Young's modulus is reduced with PHBV content. Cellulose can be considerably plasticized by the addition of PHBV.

Acknowledgements

We thank the Australian Academy of Science for awarding an ISL Scientific Visits to Europe Grant to one of us (Q.G.) to facilitate this collaboration. We also thank the Australian Institute of

Nuclear Science and Engineering (AINSE) Ltd. for funding and a PGRA scholarship to one of us (N.H.).

References

Abbott, A. P., Capper, G., Davies, D. L., Rasheed, R. H., & Tambyrajah, V. (2002). Quaternary ammonium zinc- or tin-containing ionic liquids: Water insensitive, recyclable catalysts for Diels–Alder reactions. *Green Chemistry*, *4*, 24–26.

Chan, K. L. A., Kazarian, S. G., Mavraki, A., & Williams, D. R. (2005). Fourier transform infrared imaging of human hair with a high spatial resolution without the use of a synchrotron. *Applied Spectroscopy*, *59*, 149–155.

Chiappe, C., & Pieraccini, D. J. (2005). Ionic liquids: Solvent properties and organic reactivity. *Physical Organic Chemistry*, *18*, 275–297.

Crawford, R. L. (1981). *Lignin biodegradation and transformation*. New York: John Wiley and Sons.

Dadi, A. P., Varanasi, S., & Schall, C. A. (2006). Enhancement of cellulose saccharification kinetics using an ionic liquid pretreatment step. *Biotechnology and Bioengineering*, *95*, 904–910.

Davis, J. H., Jr., & Fox, P. A. (2003). From curiosities to commodities: Ionic liquids begin the transition. *Chemical Communications*, *11*, 1209–1212.

Dupont, J., de Souza, R. F., & Suarez, P. A. Z. (2002). Ionic liquid (molten salt) phase organometallic catalysis. *Chemical Reviews*, *102*, 3667–3692.

Earle, M. J., & Seddon, K. R. (2000). Ionic liquids. Green solvents for the future. *Pure and Applied Chemistry*, *72*, 1391–1398.

El Seoud, O. A., Koschella, A., Fidale, L. C., Dorn, S., & Heinze, T. (2007). Applications of ionic liquids in carbohydrate chemistry: A window of opportunities. *Biomacromolecules*, *8*, 2629–2647.

Fei, B., Chen, C., Wu, H., Peng, S., Wang, X., Dong, L., et al. (2004). Modified poly(3-hydroxybutyrate-co-3-hydroxyvalerate) using hydrogen bonding monomers. *Polymer*, *45*, 6275–6284.

Feng, L., & Chen, Z.-I. (2008). Research progress on dissolution and functional modification of cellulose in ionic liquids. *Journal of Molecular Liquids*, *142*, 1–5.

Garrett, R. H., & Grisham, C. M. (2002). *Biochemistry* (2nd ed.). Beijing: Higher Education Press.

Gupper, A., & Kazarian, S. G. (2005). Study of solvent diffusion and solvent-induced crystallization in syndiotactic polystyrene using FT-IR spectroscopy and imaging. *Macromolecules*, *38*, 2327–2332.

Gupper, A., Wilhelm, P., Schmied, M., Kazarian, S. G., Chan, K. L. A., & Reussner, J. (2002). Combined application of imaging methods for the characterization of a polymer blend. *Applied Spectroscopy*, *56*, 1515–1523.

Hameed, N., & Guo, Q. (2008). Selective hydrogen bonding and hierarchical nanostructures in poly(hydroxyether of bisphenol A)/poly(var epsilon-caprolactone)-block-poly(2-vinyl pyridine) blends. *Polymer*, *49*, 922–933.

Hameed, N., & Guo, Q. (2009). Natural wool/cellulose acetate blends regenerated from the ionic liquid 1-butyl-3-methylimidazolium chloride. *Carbohydrate Polymers*, *78*, 999–1004.

Hameed, N., & Guo, Q. (2010). Blend films of natural wool and cellulose prepared from an ionic liquid. *Cellulose*, *17*, 803–813.

Hameed, N., Salim, N. V., & Guo, Q. (2009). Microphase separation through competitive hydrogen bonding in self-assembled A-b-B/C diblock copolymer/homopolymer complexes. *Journal of Chemical Physics*, *131*(214905), 1–12).

Huddleston, J. G., Visser, A. E., Reichert, W. M., Willauer, H. D., Broker, G. A., & Rogers, R. D. (2001). Characterization and comparison of hydrophilic and hydrophobic room temperature ionic liquids incorporating the imidazolium cation. *Green Chemistry*, *3*, 156–164.

Ibbett, R. N., Schuster, K. C., & Fasching, M. (2008). The study of water behavior in regenerated cellulosic fibers by low-resolution proton NMR. *Polymer*, *49*, 5013–5022.

Iriondo, P., Iruin, J. J., & Fernandez-Berridi, M. J. (1995). Thermal and infra-red spectroscopic investigations of a miscible blend composed of poly(vinyl phenol) and poly(hydroxybutyrate). *Polymer*, *36*, 3235–3237.

Kadokaw, J., Murakami, M., Takegaw, A., & Kaneko, Y. (2009). Preparation of cellulose–starch composite gel and fibrous material from a mixture of the polysaccharides in ionic liquid. *Carbohydrate Polymers*, *75*, 180–183.

Kaplan, D. L. (1998). *Biopolymers from renewable resources*. New York: Springer.

Kazarian, S. G., & Chan, K. L. A. (2004). FTIR imaging of polymeric materials under high-pressure carbon dioxide. *Macromolecules*, *37*, 579–584.

Kazarian, S. G., & Chan, K. L. A. (2006). Applications of ATR-FTIR spectroscopic imaging to biomedical samples. *Biochimica et Biophysica Acta*, *1758*, 858–867.

Kazarian, S. G., & Chan, K. L. A. (2010). Micro and macroattenuated total reflection Fourier transform infrared spectroscopic imaging. *Applied Spectroscopy*, *64*, 135A–152A.

Kazarian, S. G., Chan, K. L. A., & Tay, F. H. (2009). ATR-FT-IR imaging for pharmaceutical and polymeric materials: From micro to macro approaches. In R. Salzer, & H. W. Siesler (Eds.), *Infrared and Raman spectroscopic imaging* (pp. 347–375). Chichester: John Wiley & Sons, Ltd.

Kazarian, S. G., Sakellarios, N., & Gordon, C. M. (2002). High-pressure CO_2-induced reduction of the melting temperature of ionic liquids. *Chemical Communications*, *12*, 1314–1315.

Klemm, D., Heublein, B., Fink, H. P., & Bohn, A. (2005). Cellulose: Fascinating biopolymer and sustainable raw material. *Angewandte Chemie International Edition*, *44*, 3358–3393.

Kubat, J., & Pattyrante, C. (1967). Transition in cellulose in the vicinity of $-30\,^{\circ}C$. *Nature*, *215*, 390–391.

Kuimova, M. K., Chan, K. L. A., & Kazarian, S. G. (2009). Chemical imaging of live cancer cells in the natural aqueous environment. *Applied Spectroscopy*, *63*, 164–171.

Lee, S. Y. (1996). Plastic bacteria? Progress and prospects for polyhydroxyalkanoate production in bacteria. *Trends in Biotechnology*, *14*, 431–438.

Nishiyama, Y., Langan, P., & Chanzy, H. (2002). Crystal structure and hydrogen-bonding system in cellulose Iβ from synchrotron X-ray and neutron fiber diffraction. *Journal of the American Chemical Society*, *124*, 9074–9082.

Palombo, F., Shen, H., Benguigui, L. E. S., Kazarian, S. G., & Upmacis, R. K. (2009). Micro ATR-FTIR spectroscopic imaging of atherosclerosis: An investigation of the contribution of inducible nitric oxide synthase to lesion composition in ApoE-null mice. *Analyst*, *134*, 1107–1118.

Ramnial, T., Ino, D. D., & Clyburne, J. A. C. (2005). Phosphonium ionic liquids as reaction media for strong bases. *Chemical Communications*, 325–327.

Remsing, R. C., Swatloski, R. P., Rogers, R. D., & Moyna, G. (2006). Mechanism of cellulose dissolution in the ionic liquid 1-n-butyl-3-methylimidazolium chloride: A 13C and 35/37Cl NMR relaxation study on model systems. *Chemical Communications*, 1271–1273.

Salim, N. V., Hameed, N., & Guo, Q. (2009). Competitive hydrogen bonding and self-assembly in poly(2-vinyl pyridine)-block-poly(methyl methacrylate)/poly(hydroxyether of bisphenol A) blends. *Journal of Polymer Science Part B: Polymer Physics*, *47*, 1894–1905.

Salim, N. V., Hanley, T., & Guo, Q. (2010). Microphase separation through competitive hydrogen bonding in double crystalline diblock copolymer/homopolymer blends. *Macromolecules*, *43*, 7695–7704.

Sankhla, I. S., Bhati, R., Singh, A. K., & Mallick, N. (2010). Poly(3-hydroxybutyrate-co-3-hydroxyvalerate) co-polymer production from a local isolate, Brevibacillus invocatus MTCC 9039. *Bioresource Technology*, *101*, 1947–1953.

Sheldon, R. (2001). Catalytic reactions in ionic liquids. *Chemical Communications*, *23*, 2399–2407.

Song, C. E. (2004). Enantioselective chemo- and bio-catalysis in ionic liquids. *Chemical Communications*, *9*, 1033–1043.

Spring, M., Ricci, C., Peggie, D., & Kazarian, S. G. (2008). ATR-FTIR imaging for the analysis of organic materials in paint cross sections: Case studies on paint samples from the National Gallery, London. *Analytical and Bioanalytical Chemistry*, *392*, 37.

Swatloski, R. P., Spear, S. K., Holbrey, J. D., & Rogers, R. D. J. (2002). Dissolution of cellulose with ionic liquids. *Journal of the American Chemical Society*, *124*, 4974–4975.

Tay, F. H., & Kazarian, S. G. (2009). Study of petroleum heat-exchanger deposits with ATR-FTIR spectroscopic imaging. *Energy Fuels*, *23*, 4059–4067.

Toussaint, A. F., & Luner, P. (1988). The wetting properties of hydrophobically modified cellulose surfaces. In *Proc. 10th Cellulose Conf.* Syraccruse, New York, 29.5–29.6, (p. 1515).

Ueki, T., & Watanabe, M. (2008). Macromolecules in ionic liquids: Progress, challenges, and opportunities. *Macromolecules*, *41*, 3739–3749.

Updegraff, D. M. (1969). Semimicro determination of cellulose in biological materials. *Analytical Biochemistry*, *32*, 420–424.

Walker, J. (1993). *Primary wood processing: Principles and practice* (1st ed.). London: Chapman & Hall.

Wasserscheid, P., & Keim, W. (2000). Ionic liquids – new solutions for transition metal catalysis. *Angewandte Chemie International Edition*, *39*, 3772–3789.

Welton, T. (1999). Room-temperature ionic liquids. Solvents for synthesis and catalysis. *Chemical Reviews*, *99*, 2071–2084.

Wu, R. L., Wang, X. L., Li, F., Li, H. Z., & Wang, Y. Z. (2009a). Green composite films prepared from cellulose, starch and lignin in room-temperature ionic liquid. *Bioresource Technology*, *100*, 2569–2574.

Wu, R. L., Wang, X. L., Li, F., Li, H. Z., & Wang, Y. Z. (2009b). Cellulose/soy protein isolate blend films prepared via room-temperature ionic liquid. *Industrial and Engineering Chemistry Research*, *48*, 7132–7136.

Wu, B., Zhang, Y., & Wang, H. (2008). Phase behavior for ternary systems composed of ionic liquid + saccharides + water. *Journal of Physical Chemistry B*, *112*, 6426–6429.

Wu, J., Zhang, J., Zhang, H., He, J. S., Ren, Q., & Guo, M. L. (2004). Homogeneous acetylation of cellulose in a new ionic liquid. *Biomacromolecules*, *5*, 266–268.

Xie, H., King, A., Kilpelainen, I., Granstrom, M., & Argyropoulos, D. S. (2007). Thorough chemical modification of wood-based lignocellulosic materials in ionic liquids. *Biomacromolecules*, *8*, 3740–3748.

Zhang, Y., Shen, Y., Yuan, J., Han, D., Wang, Z., Zhang, Q., et al. (2006). Design and synthesis of multifunctional materials based on an ionic-liquid backbone. *Angewandte Chemie International Edition*, *35*, 5867–5870.

Zhang, H., Wang, Z., Zhang, Z., Wu, J., Zhang, J., & He, J. (2007). Regenerated-cellulose/multiwalled-carbon-nanotube composite fibers with enhanced mechanical properties prepared with the ionic liquid 1-allyl-3-methylimidazolium chloride. *Advanced Materials*, *19*, 698–704.

Zhang, H., Wu, J., Zhang, J., & He, J. (2005). 1-Allyl-3-methylimidazolium chloride room temperature ionic liquid: A new and powerful nonderivatizing solvent for cellulose. *Macromolecules*, *38*, 8272–8277.